Pharmacology Biochemistry & Behavior, Vol. 33, pp. 679–689. © Pergamon Press plc, 1989. Printed in the U.S.A. 0091-3057/89 $3.00 + .00

Variation of Nicotinic Binding Sites Among Inbred Strains

MICHAEL J. MARKS,[1] ELENA ROMM, STEPHEN M. CAMPBELL AND ALLAN C. COLLINS

Institute for Behavioral Genetics and School of Pharmacy
University of Colorado, Boulder, CO 80309

Received 8 August 1988

MARKS, M. J., E. ROMM, S. M. CAMPBELL AND A. C. COLLINS. *Variation of nicotinic binding sites among inbred strains.* PHARMACOL BIOCHEM BEHAV **33**(3) 679–689, 1989.—The specific binding of L-nicotine and α-bungarotoxin, two ligands which label different populations of putative nicotinic receptors, was determined in eight brain regions of 19 inbred mouse strains. The dissociation constants for L-nicotine (average = 2.26 nM) and α-bungarotoxin (average = 0.31 nM) did not vary significantly among the brain regions or strains. In contrast, significant variability among the maximal binding sites was observed between regions and among the strains within a region. Significant differences in L-nicotine binding were observed among the strains in midbrain, hindbrain, hippocampus, hypothalamus and colliculi, while little variability was noted in cortex or cerebellum. In general, those strains that had high L-nicotine binding in one region had high nicotine binding in the other regions. The strains clustered into two large groups: one group expressing relatively low binding and a second group expressing relatively high binding. Significant differences in α-bungarotoxin binding were observed in seven of the eight regions measured and, in general, those strains with high binding in one region tended to have high binding in the other regions. The strains clustered into three groups: those with low binding (DBA/1 and DBA/2), those with high binding (ST/b alone) and those with intermediate binding (the remaining 16 strains). The amount of binding of the two ligands did not correlate with each other. Comparison of nicotinic ligand binding with physiological response to nicotine suggests a relationship of L-nicotine binding with several responses observed after injection of low doses of nicotine and a relationship between α-bungarotoxin binding and nicotine-induced seizures.

Nicotinic cholinergic receptors Nicotine α-Bungarotoxin Pharmacogenetics

AT least two types of putative nicotinic receptors have been identified in the central nervous system of several species. One subtype of nicotinic receptor can be identified by the high affinity binding of agonists such as [^{3}H]nicotine (1, 4, 7, 12, 24, 27) or [^{3}H]acetylcholine (16, 17, 22, 26). These two ligands apparently label the same binding sites (2, 16, 17). In general, this binding site is characterized by high affinity for many nicotinic agonists, but lower affinity for nicotinic antagonists (12, 16, 17, 26). A second subtype of nicotinic receptor has been identified by the high affinity binding of the elapid neurotoxin, α-bungarotoxin (α-BTX) (9, 21, 23). Although this binding site also shows a nicotinic profile, agonists inhibit α-[^{125}I]BTX with a lower affinity than they inhibit either nicotine or ACh binding; the affinity for antagonists is comparable for the two sites (9, 12, 16).

The regional distributions of binding sites for nicotine/ACh and α-BTX differ. Receptor binding assays have demonstrated that the site densities for the two ligand types differ among the brain regions for both rats (16,26) and mice (12,16). Autoradiographic comparison of nicotine, ACh and α-BTX binding strikingly demonstrated that nicotine and ACh label the same sites, while α-BTX labels a distinctly different set of sites (2).

The molecular properties of these two binding sites also differ. While the subunit composition of the nicotinic receptor in the CNS labeled with α-BTX closely resembles that of this receptor at the neuromuscular function (3), the subunit composition of the receptor labeled with nicotine/ACh is different (28). The nicotine/ACh binding site may represent a family of related receptors (5).

Changes in the levels of these receptors may be important in mediating the development of tolerance to the effects of nicotine observed after chronic treatment with the drug. Chronic injection of rats (13, 22, 25) or chronic intravenous infusion of mice (10,16) with nicotine results in an increase in the numbers of nicotine/ACh sites. The changes are both dose (10,14) and time-dependent (13) and parallel changes in responsiveness to the drug. The binding site for α-BTX also increases with chronic nicotine infusion, but higher doses of nicotine are required to achieve the upregulation (10,14).

The influence of genotype on the level of expression of these two binding sites has also been investigated. Analysis of four inbred mouse strains failed to reveal significant differences in the levels of nicotine binding in several brain regions, but demonstrated significant variation in the expression of α-BTX in several brain regions (11). A classical genetic cross was subsequently used to investigate the heritability of these differences in receptor

[1]Requests for reprints should be addressed to Dr. Michael J. Marks, Institute for Behavioral Genetics, Campus Box 447, University of Colorado, Boulder, CO 80309.

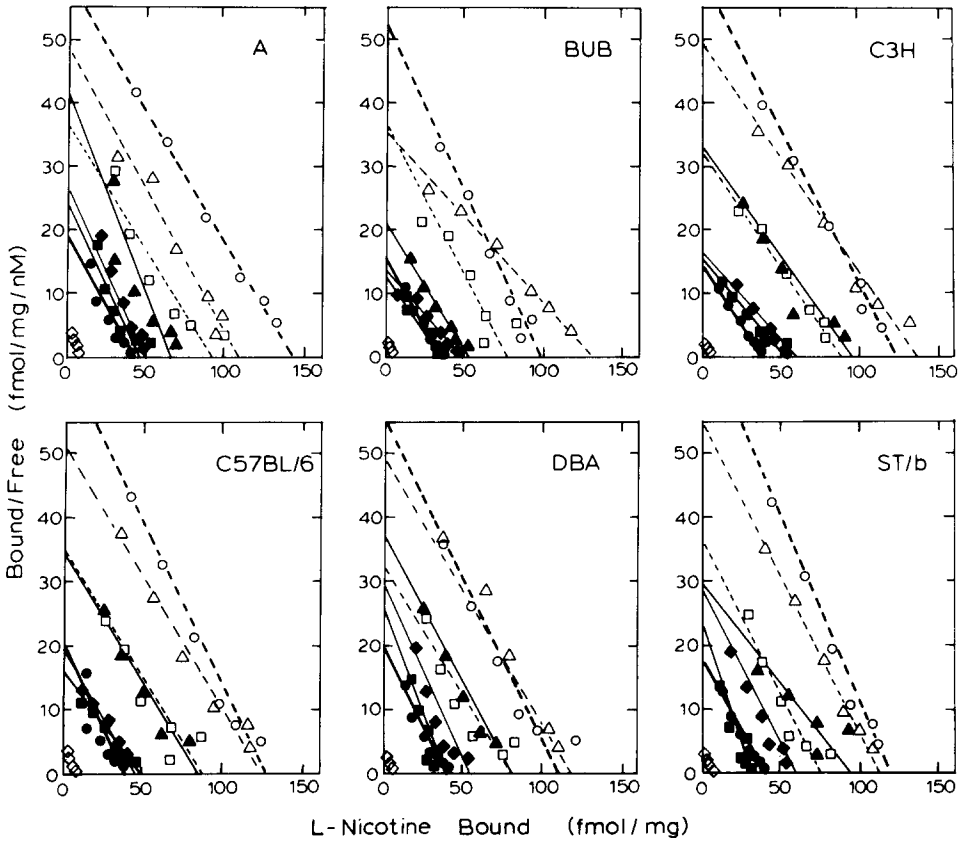

FIG. 1.Scatchard plots for L-[^{3}H]nicotine binding. Binding of L-[^{3}H]nicotine was determined for the six strains indicated using several ligand concentrations as described in the Method section. The eight brain regions assayed are represented as follows: cortex ●, midbrain ○, hindbrain ◆, cerebellum ◇, hippocampus ■, striatum □, hypothalamus ▲, and colliculi △. Each point represents the average of at least two independent experiments.

expression and indicated that for the strains used (C3H and DBA) dominance toward expression of low levels of α-BTX binding in hippocampus occurred (19,20). The analysis also suggested a relationship between hippocampal α-BTX binding and seizure sensitivity.

The success of a genetic analysis in assigning a tentative relationship between nicotinic receptor level and physiological response to the drug prompted screening of 19 inbred strains for their responsiveness to nicotine as measured by seizures (18) and by lower dose effects (15). The present study makes use of these same 19 strains and involves the measurement of the two putative nicotinic receptors in eight brain regions. The results extend the number of strains expressing differential levels of nicotinic receptors and allow a comparison of sensitivity of the mice to the physiological effects of nicotine with the number of putative nicotinic receptors in the brain.

METHOD

Animals

Male mice of 19 inbred strains were used in this study. Mice of the A/J/Ibg, C57BL/6/J/Ibg, DBA/2J/Ibg, and C3H/2Ibg strains were bred at the Institute for Behavioral Genetics, University of Colorado, Boulder, CO. These strains have been maintained at the Institute for at least 20 generations. Male mice of the BALB/cByJ strain, originally obtained from the Jackson Laboratories, Bar Harbor, ME, were also bred at the Institute, but have been maintained there for fewer than eight generations. All mice were weaned at 25 days of age and were housed with male littermates. Animals were 60–90 days old when tested. Male mice of the following strains were purchased from Jackson Laboratory, Bar Harbor, ME: AKR/J, BUB/BnJ, CBA/J, C57BL/10J, C57BR/cdJ, C57L/J, C58/J, DBA/1J, LP/J, P/J, RIIIS/J, SJL/J, ST/bJ, and SWR/J. All mice were 4–6 weeks old when they were received and were housed five per cage in our mouse colony until they were 60–90 days old. A 12-hr light/12-hr dark cycle (lights on 7 a.m. to 7 p.m.) was maintained and animals were given free access to food (Wayne Lab Blox) and water.

Materials

The radiochemicals used in this study were obtained from the following sources: L-[^{3}H]nicotine (N-methyl [^{3}H], specific activity 63.5 Ci/mmol) from Amersham Corporation, Arlington Heights, IL and α-[^{125}I]BTX (Tyr [^{125}I], initial specific activity: 132.6 Ci/mmol) from New England Nuclear, Boston, MA. Liquid L-nicotine, polyethylenimine and bovine serum albumin were purchased from Sigma Chemical Co., St. Louis, MO. The nicotine was redistilled periodically. Ultra pure [4-(2-hydroxyethyl)-1-piperazineethanesulfonic acid (HEPES)] was obtained from Boehringer-Mannheim Biochemicals, Indianapolis, IN. Glass

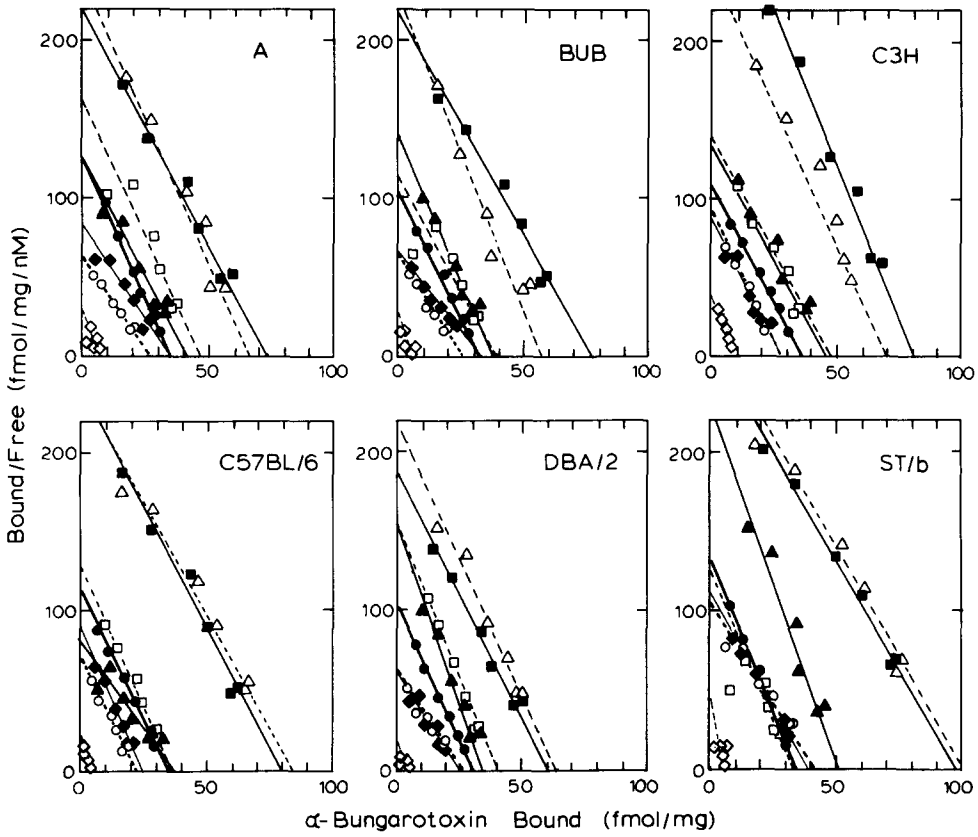

FIG. 2. Scatchard plots for α-[^{125}I]bungarotoxin binding. Binding of α-[^{125}I]BTX was determined for the six strains indicated using several ligand concentrations as described in the Method section. The eight brain regions assayed are represented as follows: cortex ●, midbrain ○, hindbrain ◆, cerebellum ◇, hippocampus ■, striatum □, hypothalamus ▲, and colliculi △. Each point represents the average of at least two independent experiments.

fiber filters were manufactured by Gelman Sciences Inc. and were obtained from American Scientific Products.

Tissue Preparation

Mice were killed by cervical dislocation. Each brain was removed and placed on an ice-cold platform. The brains were dissected into eight regions: cerebral cortex, hindbrain (pons-medulla), cerebellum, hypothalamus, striatum, hippocampus, superior and inferior colliculi, and midbrain (primarily thalamus).

After dissection, each brain region was placed in 10 volumes of ice-cold buffer (Krebs-Ringer's HEPES: NaCl, 118 mM; KCl, 4.8 mM; $MgSO_4$, 1.2 mM; $CaCl_2$, 2.5 mM; HEPES, 20 mM; pH adjusted to 7.5 with NaOH). The tissue was homogenized using a teflon pestle. The tissue preparation used was essentially that described by Romano and Goldstein (24). The homogenate was centrifuged at 18000 × g for 20 min and the pellet was resuspended in 20 volumes of distilled water. After a 60 min incubation at 4°, the pellet was collected by centrifugation at 18000 × g for 20 min. This pellet was subsequently resuspended in 10 volumes of Krebs-Ringer's HEPES and the suspension was centrifuged at 18000 × g for 20 min. The buffer was discarded and 10 volumes of fresh Krebs-Ringer's HEPES was added. The sample was then frozen at −70° until assay. Prior to each centrifugation, the sample was incubated at 37° for 10 min to promote hydrolysis of endogenous ACh.

On the day of assay, the pellet was resuspended in the overlying buffer. The sample was then incubated at 37° for 10 min after which it was centrifuged at 18000 × g for 20 min. The resulting pellet was then resuspended in Krebs-Ringer's HEPES for use in the assays.

L-[^{3}H]Nicotine Binding

The binding of L-[^{3}H]nicotine was determined using a modification of the method of Romano and Goldstein (24) as described previously (11,16). In these experiments, L-[^{3}H]nicotine binding was measured at 4°. Incubations were conducted in 12 × 75 mm polypropylene test tubes. Final incubation volume was 250 μl. The buffer used in these incubations was Krebs-Ringer's HEPES and 200 mM TRIS buffer (pH = 7.5 at 4°) was also included in the incubations. The incubation time for binding was 2 hr (equilibrium reached at 1 hr). Samples contained 100–500 μg of protein. At the completion of the incubation period, samples were filtered in the cold room using apparatus which had been cooled to 4°. The binding reaction was terminated by diluting the samples with 3 ml of ice cold buffer and followed immediately by filtration of the samples onto glass fiber filters that had been soaked overnight in

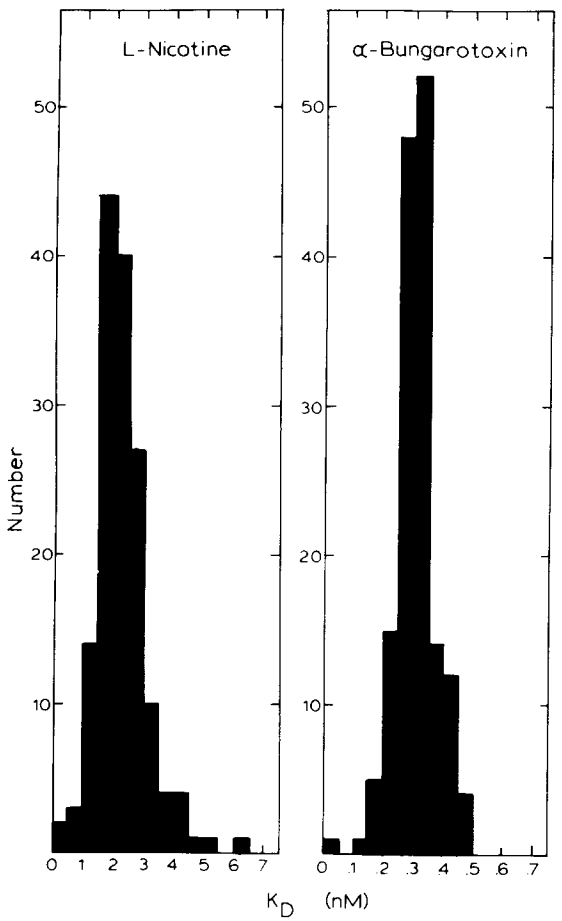

FIG. 3. Distribution of K_D values for L-[^{3}H]nicotine and α-[^{125}I]BTX. K_D values were determined from Scatchard plots for the binding of each ligand to each of 8 brain regions in the 19 inbred strains. Histograms summarize data obtained from all regions and strains.

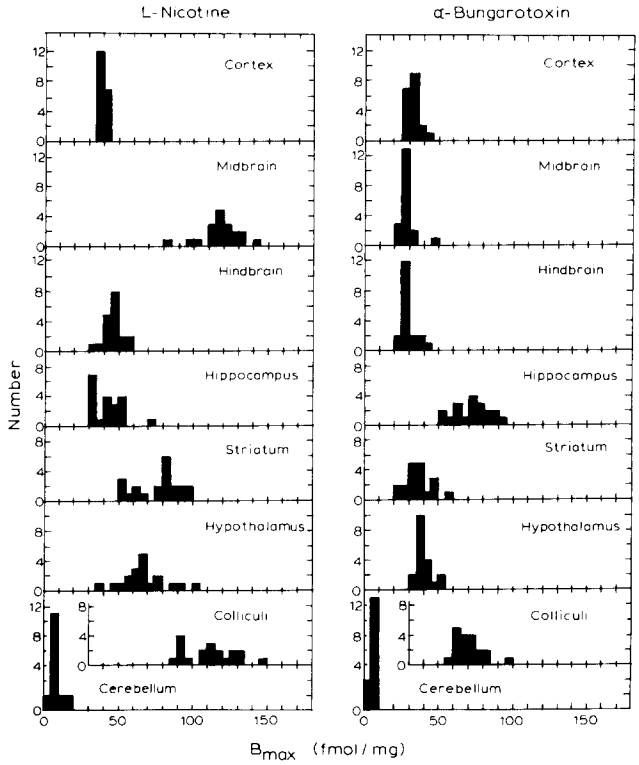

FIG. 4. Distribution of B_{max} values for L-[^{3}H]nicotine and α-[^{125}I]BTX. B_{max} values were calculated from Scatchard plots for the binding of each ligand in the 8 brain regions of the 19 inbred strains. Distribution of the B_{max} values in each of the regions is indicated by the histograms.

buffer containing 0.5% polyethylenimine. Vacuum pressure was −50 to −100 torr. Samples routinely contained approximately 5 nM L-[^{3}H]nicotine. Blanks were established by including 10 μM nicotine in the samples.

The measurements of K_D and B_{max} were accomplished both by increasing the amount of radiolabeled compound in the incubation (to a concentration of 10 nM) and by adding nonlabeled nicotine to the incubations for concentrations greater than 10 nM. The binding constants were determined by linear regression analysis of Scatchard plots of the data. Saturation curves were constructed for every brain region of each strain.

The L-[^{3}H]nicotine was repurified by thin layer chromatography before use. The chromatogram was developed using Silica Gel G and a solvent system composed of $CHCl_3$:C_2H_5OH:NH_4OH (60:40:0.1). The nicotine was extracted from the thin layer plate with ethanol and stored frozen at −70° in ethanol/water containing a 5-fold molar excess of mercaptoacetic acid.

α-[^{125}I]Bungarotoxin Binding

The binding of α-[^{125}I]BTX was measured at 37° essentially as described previously (11,16). The binding buffer was Krebs-Ringer's HEPES containing 0.1% bovine serum albumin. Binding reactions were conducted in polypropylene test tubes in an incubation volume of 500 μl. Samples contained 50–250 μg of protein. Incubations were conducted for 4 hr (equilibrium reached in 2.5 hr). The binding reaction was terminated by dilution of the sample with ice cold wash buffer and by filtration onto glass fiber filters that had been soaked in buffer containing 0.5% polyethylenimine. Wash buffer contained 0.05% polyethylenimine. The filters were washed four additional times with 3 ml aliquots of buffer. Samples routinely contained approximately 1 nM α-[^{125}I]BTX. Blanks were established by including 1 mM L-nicotine in the incubation.

The binding constants, K_D and B_{max}, were determined from experiments in which increasing amounts of α-[^{125}I]BTX were included in the incubations. Binding constants were estimated by linear regression analysis of Scatchard plots. Saturation curves were constructed for each brain region of all strains.

Determination of Radioactivity

After filtration of tissue to which [^{3}H]nicotine had been bound, the washed glass fiber filters were placed in 7 ml plastic scintillation vials and 2.5 ml of Safety Solve was added to each vial. The vials were capped and mechanically shaken. Samples were counted on a Beckman 1800 Liquid Scintillation Spectrometer. Efficiency of counting was 45% for ^{3}H.

After filtration of tissue to which α-[^{125}I]BTX had been bound, the washed filters were placed in 12 × 75 mm test tubes and

TABLE 1

L-[^{3}H]NICOTINE BINDING

Strain	Brain Region							
	Cortex	Mid-brain	Hind-brain	Hippo-campus	Striatum	Hypo-thalamus	Colli-culi	Cere-bellum
A/JIbg	24.3 ± 1.8	76.2 ± 4.2	29.8 ± 2.4	25.6 ± 1.7	45.9 ± 2.8	40.7 ± 4.1	69.4 ± 4.4	4.1 ± 0.7
AKR/J	22.7 ± 1.4	79.4 ± 4.5	27.6 ± 1.9	26.6 ± 3.2	40.1 ± 2.3	37.7 ± 3.6	68.7 ± 7.4	3.4 ± 0.6
BALB/cByJ	21.2 ± 1.1	68.4 ± 3.5	25.5 ± 1.7	23.8 ± 2.6	38.5 ± 2.0	31.5 ± 6.1	69.8 ± 8.4	4.2 ± 0.3
BUB/BnJ	22.1 ± 1.7	61.4 ± 3.4	24.3 ± 1.7	19.0 ± 1.7	36.9 ± 3.9	30.0 ± 2.2	62.3 ± 5.6	3.5 ± 0.5
CBA/J	22.4 ± 1.0	62.5 ± 5.5	23.8 ± 1.5	20.2 ± 1.9	41.7 ± 3.2	35.3 ± 1.9	56.7 ± 3.9	4.0 ± 0.4
C3H/2Ibg	22.7 ± 2.2	78.7 ± 1.8	28.9 ± 1.5	25.5 ± 1.2	46.3 ± 2.7	43.6 ± 4.8	65.4 ± 4.9	3.8 ± 0.3
C57BL/6JIbg	23.8 ± 1.9	72.0 ± 4.4	27.6 ± 2.3	26.4 ± 1.2	43.4 ± 3.0	40.6 ± 4.8	65.4 ± 4.9	4.8 ± 0.5
C57BL/10J	24.9 ± 1.9	80.9 ± 4.2	32.8 ± 1.4	28.7 ± 2.0	45.6 ± 2.9	37.2 ± 4.3	69.1 ± 5.5	5.4 ± 0.4
C57BR/cdJ	22.3 ± 1.3	75.4 ± 5.3	30.9 ± 2.4	25.1 ± 2.3	50.6 ± 4.1	47.7 ± 3.0	82.8 ± 4.9	3.9 ± 0.6
C57L/J	21.5 ± 2.1	66.1 ± 5.4	27.7 ± 1.5	28.5 ± 1.5	42.0 ± 2.2	40.9 ± 3.2	72.5 ± 5.8	4.2 ± 0.9
C58/J	23.4 ± 1.9	71.6 ± 3.6	26.4 ± 1.0	20.1 ± 1.3	38.5 ± 1.4	27.4 ± 1.7	53.6 ± 3.8	4.7 ± 0.3
DBA/1J	22.4 ± 1.8	66.4 ± 3.8	25.6 ± 2.0	25.3 ± 1.9	41.7 ± 2.6	33.4 ± 4.0	60.3 ± 3.7	4.9 ± 0.7
DBA/2JIbg	24.8 ± 1.5	73.0 ± 1.4	31.3 ± 2.6	24.4 ± 0.9	45.1 ± 0.8	41.7 ± 4.4	64.8 ± 4.7	3.8 ± 0.3
LP/J	23.7 ± 0.9	73.1 ± 3.1	26.2 ± 1.2	18.8 ± 1.7	36.7 ± 2.3	34.9 ± 3.5	56.6 ± 3.4	4.4 ± 0.5
P/J	25.3 ± 1.6	77.5 ± 5.8	30.1 ± 1.5	23.2 ± 1.8	47.3 ± 2.6	41.8 ± 3.7	71.0 ± 3.9	5.0 ± 0.5
RIIIS/J	20.9 ± 1.8	63.0 ± 4.9	25.6 ± 1.5	22.7 ± 1.6	43.4 ± 3.3	32.7 ± 2.2	66.9 ± 5.1	3.7 ± 0.7
SJL/J	23.1 ± 2.0	67.6 ± 3.0	28.7 ± 2.4	24.3 ± 1.9	42.4 ± 2.7	37.4 ± 1.9	67.9 ± 5.1	5.3 ± 0.8
ST/bJ	22.7 ± 2.4	77.7 ± 4.3	32.8 ± 2.0	23.9 ± 3.2	40.1 ± 3.8	38.7 ± 4.1	76.9 ± 6.5	5.9 ± 0.8
SWR/J	21.4 ± 2.0	65.7 ± 4.8	25.1 ± 1.8	22.3 ± 1.8	44.2 ± 3.9	36.4 ± 4.7	59.3 ± 5.6	4.8 ± 0.8
One-way Results	F(18,134) = 0.59	F(18,123) = 2.15†	F(18,127) = 2.13†	F(18,125) = 2.07*	F(18,130) = 1.57	F(18,128) = 1.71*	F(18,124) = 1.77*	F(18,132) = 1.40

L-[^{3}H]nicotine binding was measured in eight brain regions of 6–9 individual mice of the 19 strains using an average ligand concentration of 4.3 nM. Results shown are mean ± SEM. Binding values are expressed as fmol/mg protein. Results of the one-way ANOVAs are given at the bottom of the column for the appropriate region: *$p<0.05$, †$p<0.01$.

radioactivity determined using a Packard 5000 Series Gamma Counter. Counting efficiency was 80%.

Protein Assay

Protein was measured using the method of Lowry *et al.* (8) with bovine serum albumin as the standard.

Statistical Analysis

Scatchard plots for binding data were analyzed by linear regression and the binding parameters, K_D and B_{max}, were calculated from the resulting equations.

The Statistical Package for the Social Sciences (SPSSPC), adapted for use on the personal computer, was used for all of the other statistical analyses. Binding data obtained from single point assays were analyzed using Analysis of Variance (ANOVA) both as a function of strain and brain region and by one-way ANOVA within a region as a function of strain. Differences among the strains were tested using Duncan's new multiple range test.

Possible relationships of the binding site densities for the two ligands in the eight brain regions were assessed using regression analysis.

The binding of each ligand in the eight regions was further analyzed using factor analysis. The data were analyzed using principle components analysis to extract the factors and the factors were subsequently subjected to varimax rotation. Other extraction and rotation methods gave similar results.

Cluster analysis was used to group the strains into groups expressing similar numbers of putative nicotinic receptors. The primary method of cluster formation made use of squared Euclidian distances between groups and the minimum average linkage between groups was used to combine clusters. Cluster analysis for L-[^{3}H]nicotine binding employed the data from the following six brain regions: midbrain, hindbrain, hippocampus, striatum, hypothalamus, and striatum. Cluster analysis for α-[^{125}I]BTX employed the data from the following brain regions: cortex, midbrain, hindbrain, hippocampus, hypothalamus, and colliculi. The regions were chosen for cluster analysis because they all shared a single factor as extracted by the principle components analysis. Cluster analyses using actual binding data and data normalized within a region were similar.

RESULTS

Saturation Curves for Nicotinic Ligand Binding

Saturation curves were constructed for the binding of L-[^{3}H]nicotine and α-[^{125}I]BTX in each of eight brain regions (cortex, hippocampus, striatum, hypothalamus, combined inferior and superior colliculi, cerebellum, hindbrain and midbrain). Scatchard plots for the binding of L-[^{3}H]nicotine and for the binding of

TABLE 2

α-[^{125}I]BTX BINDING

Strain	Brain Region							
	Cortex	Mid-brain	Hind-brain	Hippo-campus	Striatum	Hypo-thalamus	Colli-culi	Cere-bellum
A/JIbg	26.0 ± 0.9	19.6 ± 1.0	21.3 ± 2.0	56.4 ± 2.9	31.7 ± 2.5	33.0 ± 3.3	62.7 ± 5.5	5.5 ± 0.9
AKR/J	20.8 ± 0.9	26.7 ± 4.3	21.6 ± 1.4	48.5 ± 2.0	24.5 ± 1.3	30.4 ± 3.9	58.8 ± 1.9	4.3 ± 0.7
BALB/cByJ	21.3 ± 1.1	16.5 ± 1.0	20.7 ± 1.0	50.8 ± 1.9	23.4 ± 1.4	31.1 ± 2.0	54.2 ± 2.6	5.4 ± 0.5
BUB/BnJ	23.7 ± 1.3	19.5 ± 1.7	21.8 ± 1.0	65.3 ± 6.8	21.5 ± 1.3	31.1 ± 2.0	52.3 ± 3.0	5.4 ± 0.4
CBA/J	24.7 ± 1.0	16.2 ± 1.0	19.8 ± 1.1	55.1 ± 3.0	27.2 ± 1.9	30.9 ± 3.8	57.3 ± 3.1	5.3 ± 0.8
C3H/2Ibg	26.0 ± 1.1	20.9 ± 1.2	20.9 ± 1.5	69.2 ± 4.2	31.2 ± 1.8	35.4 ± 0.9	62.1 ± 3.0	5.8 ± 0.7
C57BL/6JIbg	25.4 ± 0.9	17.9 ± 1.0	20.0 ± 0.7	59.3 ± 4.5	28.4 ± 1.5	39.5 ± 4.5	58.7 ± 3.0	4.0 ± 0.6
C57BL/10J	27.6 ± 1.1	23.4 ± 2.0	21.5 ± 1.4	63.6 ± 2.5	26.7 ± 1.8	30.7 ± 2.4	51.2 ± 1.6	6.9 ± 0.4
C57BR/cdJ	26.6 ± 1.4	20.5 ± 1.7	22.5 ± 1.2	65.0 ± 1.7	26.2 ± 1.3	35.6 ± 1.3	64.3 ± 4.3	6.6 ± 0.5
C57L/J	24.0 ± 1.1	21.0 ± 1.6	23.3 ± 1.5	53.5 ± 1.6	25.3 ± 1.4	34.4 ± 3.4	57.3 ± 2.7	5.4 ± 0.9
C58/J	31.4 ± 0.6	22.2 ± 1.3	24.5 ± 1.4	68.5 ± 4.3	27.7 ± 2.0	36.6 ± 3.7	57.6 ± 3.2	6.6 ± 0.5
DBA/1J	22.1 ± 0.5	16.8 ± 1.3	19.3 ± 1.6	42.8 ± 2.8	30.2 ± 2.2	26.2 ± 2.5	47.4 ± 3.0	3.8 ± 0.8
DBA/2JIbg	23.4 ± 1.0	18.5 ± 0.7	19.7 ± 1.6	45.6 ± 2.2	37.6 ± 3.5	31.2 ± 2.0	46.9 ± 3.7	3.0 ± 0.4
LP/J	26.2 ± 0.7	19.5 ± 1.0	20.6 ± 1.7	53.9 ± 2.7	32.9 ± 3.6	33.5 ± 3.4	48.5 ± 1.7	5.6 ± 0.8
P/J	22.0 ± 0.7	20.3 ± 1.6	20.4 ± 1.3	54.1 ± 2.3	27.1 ± 2.4	36.8 ± 3.8	57.2 ± 3.0	7.0 ± 0.8
RIIIS/J	22.4 ± 1.3	21.5 ± 0.9	21.3 ± 1.3	56.9 ± 4.2	23.1 ± 2.8	31.6 ± 3.0	53.5 ± 6.4	5.6 ± 0.8
SJL/J	25.6 ± 1.5	21.5 ± 0.9	19.7 ± 2.0	64.0 ± 3.8	24.9 ± 2.1	31.8 ± 3.2	56.9 ± 2.6	4.3 ± 0.5
ST/bJ	26.9 ± 1.5	27.2 ± 1.8	27.0 ± 1.3	74.4 ± 3.7	27.9 ± 2.0	41.1 ± 3.2	79.6 ± 3.6	3.5 ± 0.3
SWR/J	19.9 ± 0.3	23.3 ± 3.6	18.2 ± 1.0	52.8 ± 2.1	21.5 ± 1.4	31.7 ± 2.8	54.6 ± 5.8	3.4 ± 0.5
One-Way Results	All Analyses Degrees of Freedom = 18,133							
	F = 7.18‡	F = 2.48†	F = 2.05*	F = 5.78‡	F = 3.72‡	F = 1.43	F = 4.20‡	F = 3.39‡

The binding of α-[^{125}I]BTX was measured in the 8 brain regions of the 19 mouse strains using a 1.1 nM concentration of α-[^{125}I]BTX. Each table entry represents the mean ± SEM of 8 separate measurements. Units of binding are fmol/mg protein. The results of the one-way ANOVAs are provided at the bottom of the appropriate column. *$p<0.05$, †$p<0.01$, ‡$p<0.001$.

α-[^{125}I]BTX for six representative strains are shown in Figs. 1 and 2, respectively.

The B_{max} for the binding of L-[^{3}H]nicotine varied substantially among the brain regions in each of the six strains shown in Fig. 1. Binding in cerebellum was lowest, while that in midbrain was highest. Although B_{max} values varied substantially among the regions, the K_D values were similar as indicated by the parallelism of the Scatchard plots.

The pattern of L-[^{3}H]nicotine binding in the eight brain regions of all 19 inbred strains assayed was similar to that observed for the six representative strains in that B_{max} values varied substantially among the regions while K_D values did not. The distribution of K_D values measured in the regions is presented in the histogram in the left panel of Fig. 3. The average K_D value for L-[^{3}H]nicotine observed for all strains and brain regions was 2.26 nM. The average K_D in each of the eight brain regions was similar to this value (cortex, 2.5 nM; midbrain, 2.1 nM; hindbrain, 2.2 nM; hippocampus, 2.7 nM; striatum, 2.3 nM; hypothalamus, 2.1 nM; cerebellum, 2.0 nM; and colliculi, 2.2 nM). Eight of the 12 most divergent K_D values were measured in cerebellum, the brain region with the lowest level of nicotine binding.

The distribution of B_{max} values for L-[^{3}H]nicotine binding in the eight brain regions is summarized in the histograms in the left panel of Fig.4. The distribution of B_{max} values for the 19 strains is similar to that observed for the six representative strains as indicated in Fig.1. B_{max} values measured in cortex and cerebellum show little variation, while the B_{max} values measured in the other regions showed relatively wide variation. Although the overall average B_{max} measured in cortex was similar to that measured in hippocampus, binding was much more heterogeneous in the latter region.

The Scatchard plots shown in Fig. 2 for six representative strains indicate that the B_{max} values for α-[^{125}I]BTX varied markedly among the brain regions, with cerebellum showing the lowest binding and hippocampus or colliculi showing the highest. The Scatchard plots for α-[^{125}I]BTX binding shown in Fig. 2 are parallel, indicating that K_D values did not differ among the strains and brain regions depicted.

The pattern of α-[^{125}I]BTX binding in the eight brain regions of all 19 inbred strains assayed was similar to those shown for the six representative strains in that the B_{max} values varied substantially among the brain regions, while the K_D values did not. The distribution of K_D values for α-[^{125}I]BTX in all eight brain regions of the 19 strains is indicated in the histogram in the right panel of Fig. 3. The average K_D value for α-[^{125}I]BTX binding was 0.31 nM. The average K_D value for α-[^{125}I]BTX binding was similar in each of the eight brain regions (cortex, 0.31 nM; midbrain, 0.37 nM; hindbrain 0.36 nM; hippocampus, 0.31 nM; striatum, 0.30 nM; hypothalamus, 0.29 nM; cerebellum, 0.24 nM; and colliculi, 0.29 nM). As was the case for nicotine binding, the brain region with the lowest level of α-[^{125}I]BTX binding (cerebellum), contributed many of the most divergent values (7 of 20).

The distribution of B_{max} values for α-[^{125}I]BTX binding in the eight brain regions is summarized in the histograms in the right panel of Fig. 4. The distribution of B_{max} values for the 19 strains is similar to that observed for the six representative strains as indicated in Fig. 2. B_{max} values measured in hippocampus, striatum, and colliculi showed relatively wide variation, but some variability in B_{max} values was observed in the other brain regions as well.

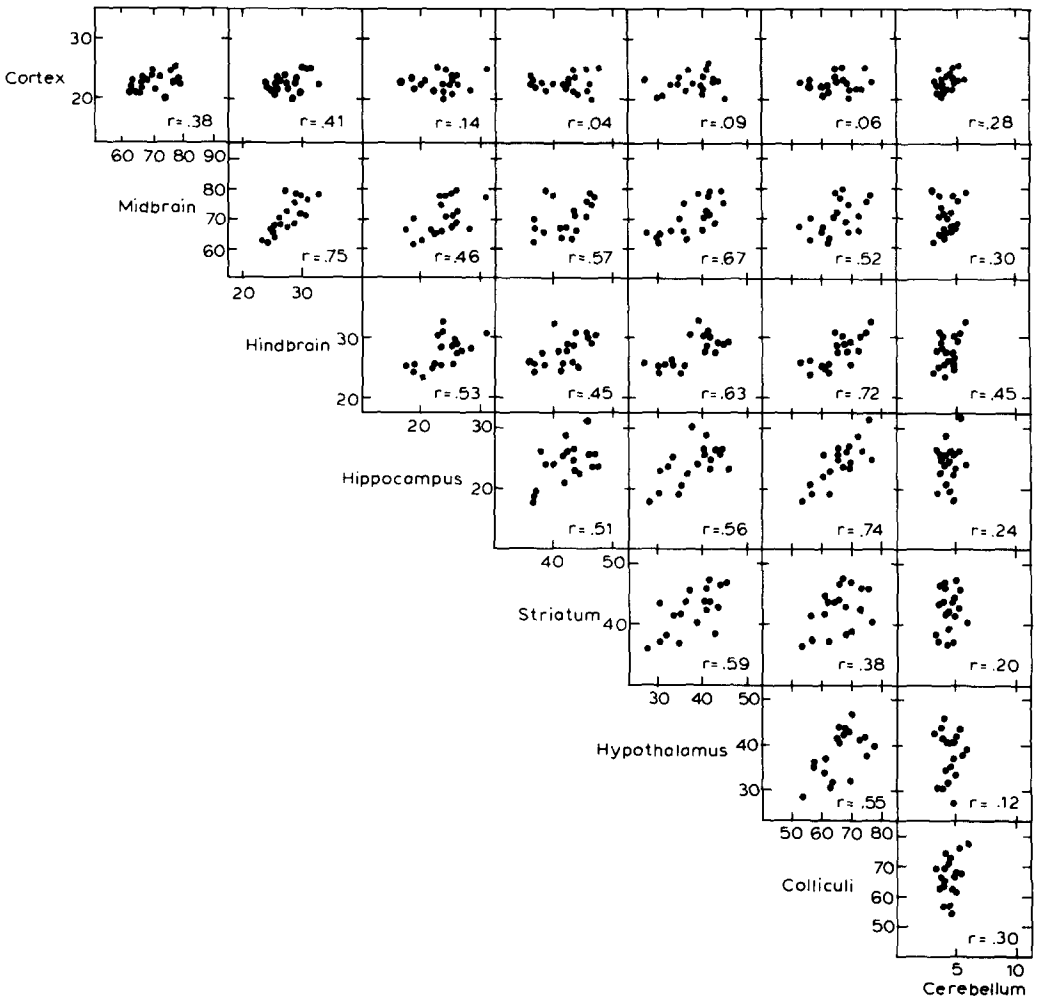

FIG. 5. Correlations of L-[^{3}H]nicotine binding among brain regions. Scattergrams of L-[^{3}H]nicotine measured in each brain regions using single point assays are presented. Each point represents the ligand binding for a given strain in the two regions listed on the axes. Correlation coefficients are indicated in each individual panel.

Comparison of Nicotinic Ligand Binding by Region and Strain

In order to increase the power of the analysis for comparison of the levels of nicotinic binding sites among the strains, binding of both L-[^{3}H]nicotine and α-[^{125}I]BTX was measured in all the brain regions of the 19 strains using a single concentration of each ligand. The relative constancy of K_D values among the strains and brain regions indicated that the results obtained using single point assays would be similar to those measured as B_{max} values from Scatchard plots. The correlation between B_{max} values and binding measured at a single concentration of L-[^{3}H]nicotine (4.3 nM) or α-[^{125}I]BTX (1.1 nM) was calculated to determine whether results of single point assays corresponded to B_{max} values. The relationship between B_{max} values and binding measured at a single concentration of ligand was highly significant for both L-[^{3}H]nicotine, r(150) = .95, and α-[^{125}I]BTX, r(150) = .98. The highly significant correlations obtained indicated that measurement of either L-[^{3}H]nicotine or α-[^{125}I]BTX binding using a single concentration of ligand provides a good estimate of the relative B_{max} values for both nicotinic ligands.

The binding of L-[^{3}H]nicotine measured using a single concentration of ligand in eight brain regions of the 19 inbred strains is summarized in Table 1. The variation in binding among the brain regions that was illustrated in Fig. 4 is confirmed by the results shown in Table 1. The lowest binding was observed in cerebellum, while highest binding occurred in midbrain and colliculi. Binding in each of the brain regions were analyzed by one-way ANOVA. No differences in binding of L-[^{3}H]nicotine occurred among the strains in either cortex or cerebellum, but significant variation occurred in midbrain, hindbrain, hippocampus, hypothalamus and colliculi. The strain differences in binding of L-[^{3}H]nicotine in striatum approached significance ($p = 0.053$).

The binding of α-[^{125}I]BTX measured using a single ligand concentration in eight brain regions of 19 inbred strains is summarized in Table 2. The variation in binding among the strains and brain regions that was illustrated in Fig. 4 is confirmed by the results presented in Table 2. The binding of α-[^{125}I]BTX was lowest in cerebellum and highest in hippocampus and colliculi. Strain differences in binding in each of the brain regions were analyzed using one-way ANOVA. Significant variation in α-[^{125}I]BTX binding among the 19 inbreds was observed for every brain region except hypothalamus.

Factor Analysis of Nicotinic Ligand Binding

The measurement of nicotinic ligand binding in several brain

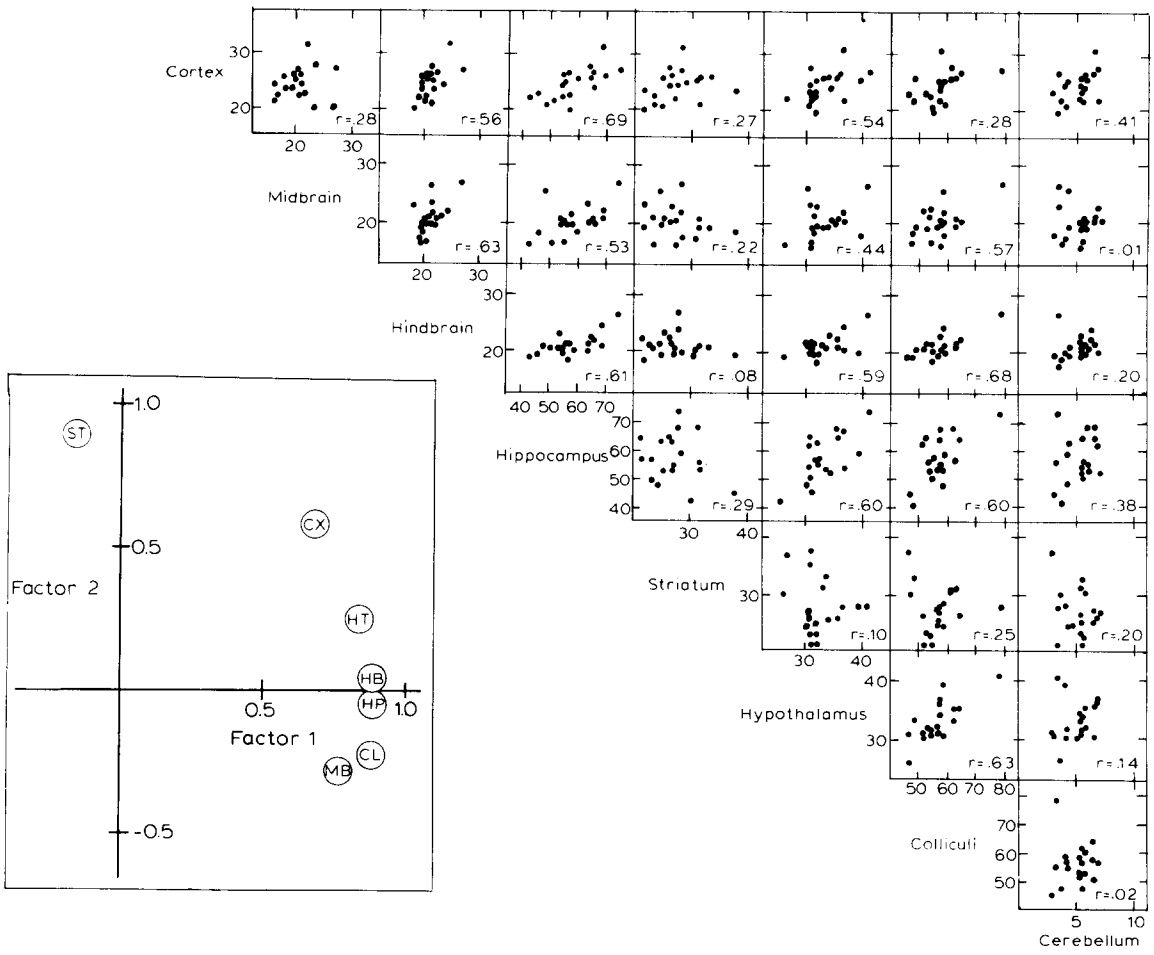

FIG. 6. Correlations of α-[^{125}I]BTX binding among brain regions. Scattergrams of α-[^{125}I]BTX measured in each brain regions using single point assays are presented in the upper right of the figure. Each point represents the ligand binding in a given strain in the two regions listed on the axes. Correlation coefficients are given in each individual panel. The panel in the lower right of the figure represents the factor loadings calculated for seven brain regions (excluding cerebellum) for the two-factor model calculated from the principle components analysis after subjection to varimax rotation.

regions of many strains allows the data to be subjected to further analysis. In order to determine whether relationships in ligand binding occurred among the brain regions, scattergrams were constructed to examine the relationship for L-[^{3}H]nicotine binding (Fig. 5) and α-[^{125}I]BTX binding (Fig. 6) in the eight brain regions.

As illustrated in Fig. 5, correlations among the binding sites for L-[^{3}H]nicotine in the eight brain regions vary. In general, the interregional correlations were lower when the comparisons involved cortex and cerebellum. Inasmuch as L-[^{3}H]nicotine binding did not vary significantly among the strains for these two regions, the absence of substantial covariance between the binding in these two regions and that in the other six regions is not unexpected. Positive correlations among the binding sites in the remaining six brain regions were observed (range from a low of $r = .38$ to a high of $r = .75$).

The existence of positive correlations among the sites indicates that the application of factor analysis would be of value. This analysis was applied to the data to determine if a simplified relationship among the binding sites may be postulated. In general, a factor analysis assumes that correlations among several variables occur because these variables are all influenced by relatively few underlying common variables, called factors. The goal of the analysis is to describe a set of experimental observations with as few underlying factors as possible. The resulting simplification of a complex set of observations may be useful in categorizing the observations and understanding the possible relationships among them. When data for L-[^{3}H]nicotine binding in midbrain, hindbrain, hippocampus, striatum, hyothalamus and colliculi of the 19 strains was subjected to principle components analysis a single factor was extracted. This factor had an eigen value of 3.72 and accounted for 62.1% of the variance for the binding of this ligand among the strains in the six brain regions. Binding in midbrain was less well explained than that in the other brain regions (49% of variance accounted for in midbrain, 61% to 71% accounted for in remaining regions).

As illustrated in Fig. 6, correlations among the number of α-[^{125}I]BTX binding sites in the brain regions vary. Binding in cerebellum, the region with the fewest α-[^{125}I]BTX binding sites, is not highly correlated with the binding in the other brain regions. In addition, α-[^{125}I]BTX binding in striatum is not highly correlated with the binding of this ligand in the other brain regions assayed. In contrast to the pattern observed for cerebellum and striatum, positive correlations in binding among the other six brain regions were observed.

The large number of significant correlations among the binding

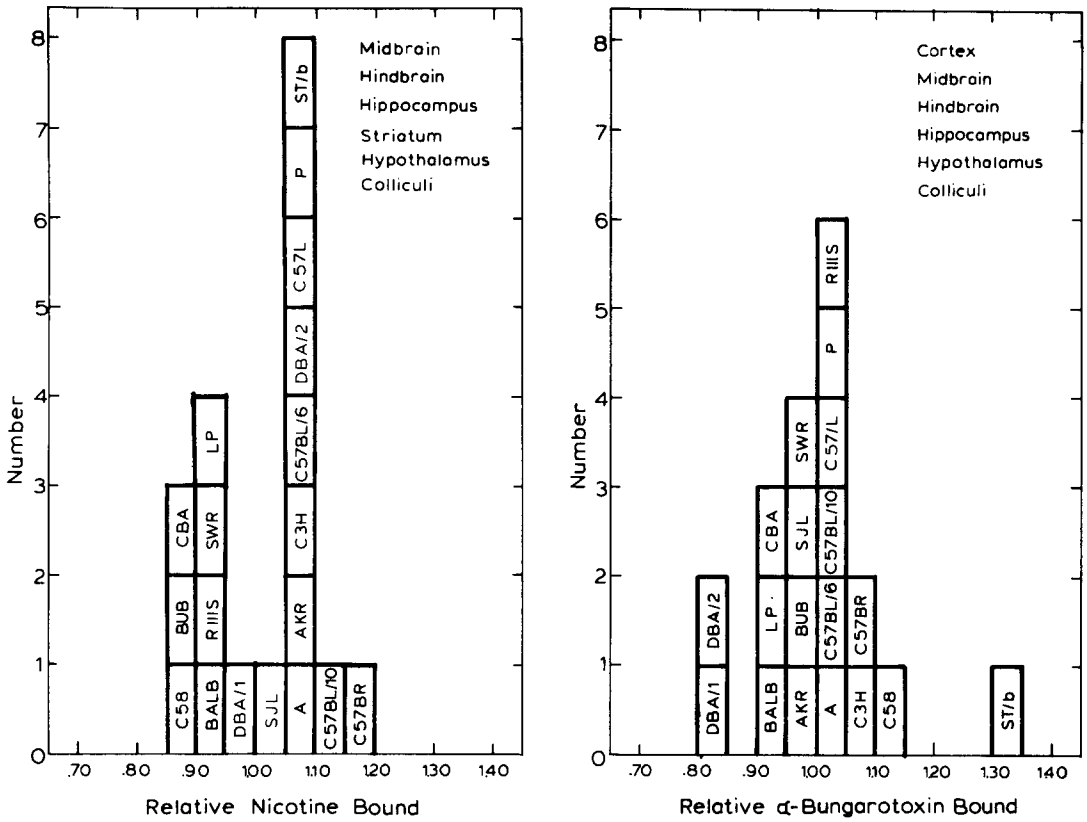

FIG. 7. Cluster analysis of nicotinic binding sites. Distribution of overall binding in the 19 inbred strains is shown for L-[^{3}H]nicotine in the left panel and for α-[^{125}I]BTX in the right panel. Values for ligand binding represent the arithmetic average of relative binding in six brain regions listed in each panel. This calculation was used to assign a single number to the binding data of each ligand for each strain for those brain regions weighting heavily on a single factor as determined by the principle components analysis. Cluster analysis of binding data for the regions individually yielded similar pattern.

sites indicated that the application of a factor analysis would be useful. The inset to Fig. 6 displays the factor loadings observed for the principle components analysis of α-[^{125}I]BTX binding in seven brain regions (cerebellum excluded). The analysis extracted two factors: the first had an eigen value of 3.83 and accounted for 53% of the variance, the second had an eigen value of 1.33 and accounted for 19% of the variance. Binding in five brain regions weighted heavily on Factor 1, while binding in striatum weighted heavily on Factor 2. Binding in cortex shared weightings with both factors. Reanalysis of the results omitting data for α-[^{125}I]BTX binding in striatum produced a one-factor solution (eigen value = 3.83 accounting for 64% of the variance). Cortical α-[^{125}I]BTX binding was the most poorly explained by a one-factor model (50% of the variance).

Cluster Analysis of Nicotinic Binding

Since factor analysis indicated that the pattern of L-[^{3}H]nicotine binding was similar in six brain regions (midbrain, hindbrain, hippocampus, hypothalamus, striatum and colliculi) and that the pattern of α-[^{125}I]BTX binding was similar in six brain regions (cortex, midbrain, hindbrain, hippocampus, hypothalamus, and colliculi), cluster analysis was used to group strains with similar overall binding of L-[^{3}H]nicotine and α-[^{125}I]BTX in the regions showing similar factor loadings. Histograms were constructed to provide a simplied presentation of ligand binding in each of the 19 strains by calculating the relative binding of the appropriate ligand in each of the brain regions grouped together by the factor analyses described above. Each mouse strain was thereby assigned a single value for either L-[^{3}H]nicotine or α-[^{125}I]BTX binding. The histograms for relative nicotinic ligand binding in the 19 strains are shown in Fig. 7.

The distribution of overall normalized L-[^{3}H]nicotine binding in midbrain, hindbrain, hippocampus, hypothalamus, striatum and colliculi in the 19 inbred strains appears to be bimodal. One group of strains displayed relatively low binding and a second group displayed relatively high binding. Cluster analysis was undertaken using the individual values for each of the six regions. The grouping of the strains was subsequently tested using cluster analysis. The cluster analysis is designed to combine into groups those strains displaying the most similarity in their expression of the nicotinic binding sites and thereby identify those strains most closely resembling each other in receptor expression. The cluster analysis grouping normalized data from all six regions confirmed the visual pattern obtained using the combined L-[^{3}H]nicotine binding shown in Fig. 7. Two large clusters were indicated, a cluster displaying relatively low nicotine binding (mean relative binding = 0.927) consisting of C58, BUB, CBA, BALB, RIIIS, SWR, LP, DBA/1 and SJL and a cluster displaying relatively high nicotine binding (mean relative binding = 1.077) consisting of A, AKR, C3H, C57BL/6, DBA/2, C57L, P, ST/b, C57BL/10 and C57BR). The cluster pattern obtained using untransformed binding data for the six brain regions, in which more weight is assigned to regions displaying higher L-[^{3}H]nicotine binding, was nearly

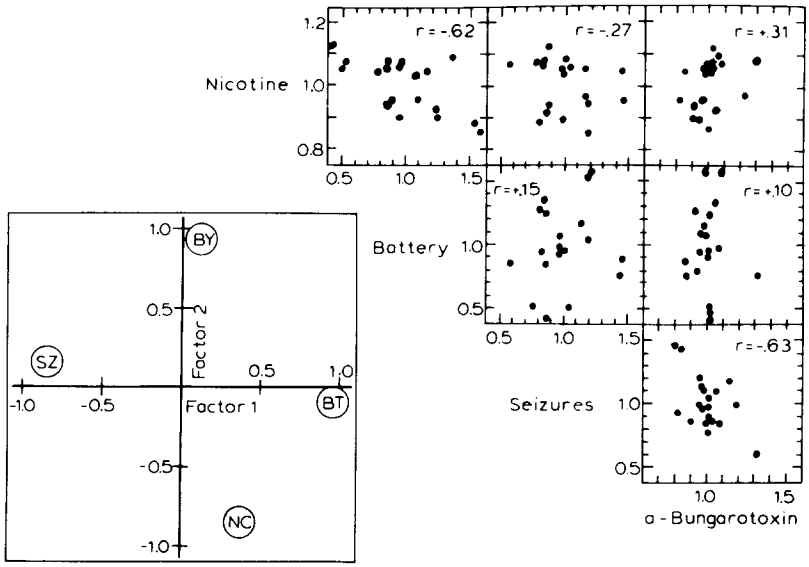

FIG. 8. Global factor analysis of physiological tests and nicotinic binding. Four measures of nicotinic responsiveness were calculated for each strain as described in the Method section. The panels in the upper right display scattergrams correlating overall nicotine binding (NB), overall low dose nicotine responsiveness (TB), overall seizure sensitivity (SS), and overall BTX binding (BB) for the 19 inbred strains tested. Correlation coefficients are listed in the panels. The panel in the lower left of the figure represents the factor loadings for each of these global measures as determined by principle components analysis after varimax rotation.

identical to that obtained with the normalized data. The only difference seen was SJL mice were assigned to the group with higher L-[^{3}H]nicotine binding.

The distribution of normalized α-[^{125}I]BTX binding obtained by combining data from six brain regions grouped together by factor analysis (cortex, midbrain, hindbrain, hippocampus, hypothalamus and colliculi) of the 19 strains was more nearly normally distributed than that for L-[^{3}H]nicotine. A large group of strains clustered about the average, two strains (DBA/1 and DBA/2) had apparently low binding and one strain (ST/b) had apparently high binding. Cluster analysis using the ungrouped data from the six brain regions was performed. The general grouping of the strains achieved using cluster analysis with both normalized and untransformed data was similar to that presented in Fig. 7 for the combined, normalized data.

DISCUSSION

The results presented in this study provide information about the regional distribution and relative site densities for the binding of two putative nicotinic receptor ligands in the brains of 19 inbred mouse strains. The results indicate that the K_D values for both L-[^{3}H]nicotine and α-[^{125}I]BTX binding show little variation from brain region to brain region and from strain to strain. In contrast, the binding site densities, B_{max} values, differ substantially from brain region to brain region. Regional variation in the amounts of putative nicotinic receptors of both the α-BTX type and the nicotine (nicotinic ACh) type has been reported previously (2, 12, 16, 26). The results presented in this paper also demonstrate that substantial variation in the amount of nicotinic ligand binding occurs within a brain among different mouse strains. The examination of 19 inbred strains extends substantially the information previously reported for nicotinic ligand binding in inbred mouse strains (11).

In general, interregional correlations in the expression of L-[^{3}H]nicotine were relatively high as were interregional correlations in the expression of α-[^{125}I]BTX sites, but the binding site densities of L-[^{3}H]nicotine did not correspond to those of α-[^{125}I]BTX; the expression of these two binding sites appears to be independent. For example, relative L-[^{3}H]nicotine binding in C58 mice is low but α-[^{125}I]BTX binding is high, but for C57BR mice binding of both ligands is relatively high, and for DBA/2 mice L-[^{3}H]nicotine binding is relatively high but α-[^{125}I]BTX binding is very low. Since these two nicotinic ligands label distinctly different putative receptors in rodent brain (2, 11, 16, 17, 26), the absence of correlation between them is no surprise.

The availability of physiological and behavioral data on the sensitivity to the effects of nicotine of the 19 inbred strains presented previously (15,18) and the availability of data on site densities of putative nicotinic receptors presented here makes the assessment of a possible relationship among these variables possible. The information presented in Fig. 8 represents a global analysis of the possible relationship among the physiological responses to nicotine and the number of brain nicotinic sites. Scattergrams relating nicotine binding, α-BTX binding, overall responsiveness of three closely related tests (Y-maze crosses and rears and body temperature, the "three test response"), and overall seizure sensitivity are shown in the upper right portion of the figure. Two significant correlation coefficients were found: 1) between nicotine binding and the "three test response" ($r = -.62$, $p = 0.005$) and 2) between α-BTX binding and seizure sensitivity ($r = -.63$, $p = 0.004$). The loadings obtained after factor analysis are represented in the lower left of Fig. 8. Two factors were extracted, one weighing heavily on α-BTX binding and negatively on seizure response, and a second weighing heavily on the "three test response" and negatively on nicotine binding. This analysis suggests a general relationship between nicotine binding and nicotine response measured by depression of activity and body temperature and a second general relationship between α-BTX binding and seizure sensitivity. Note that these relationships are expressed in the most general of terms since the variables used in the factor analysis were obtained by combining many, albeit

related, variables. Nevertheless, the intriguing suggestion of a relationship between two independent types of nicotinic receptors and two different types of in vivo responses to nicotine provides a basis to investigate further the role of nicotinic receptors in controlling these responses to nicotine in mice.

ACKNOWLEDGEMENTS

This work was supported by grant DA 03194 from the National Institute on Drug Abuse. A. C. Collins is supported, in part, by a Research Scientist Development Award (DA00116).

REFERENCES

1. Abood, L. G.; Reynolds, D. T.; Bidlack, J. M. Stereospecific ^{3}H-nicotine binding to intact and solubilized rat brain membranes and evidence for its noncholinergic nature. Life Sci. 27:1307–1314; 1980.
2. Clarke, P. B. S.; Schwartz, R. D.; Paul, S. M.; Pert, C. B.; Pert, A. Nicotinic binding in rat brain: autoradiographic comparison of [^{3}H]acetylcholine, [^{3}H]nicotine, and [^{125}I]-α-bungarotoxin. J. Neurosci. 5:1307–1315; 1985.
3. Conti-Tronconi, B. M.; Dunn, S. M. J.; Barnard, E. A.; Dolly, J. O.; Lai, F. A.; Ray, N.; Raftery, M. A. Brain and muscle nicotinic acetylcholine receptors are different but homologous proteins. Proc. Natl. Acad. Sci. USA 82:5208–5212; 1985.
4. Costa, L. G.; Murphy, S. D. [^{3}H]Nicotine binding in rat brain: alteration after chronic acetylcholinesterase inhibition. J. Pharmacol. Exp. Ther. 226:392–397; 1983.
5. Goldman, D.; Deneris, E.; Luyten, W.; Kochhar, A.; Patrick, J.; Heinemann, S. Members of a nicotinic acetylcholine receptor gene family are expressed in different regions of mammalian central nervous system. Cell 48:965–973; 1987.
6. Kemp, G.; Morley, B. J. Ganglionic nAChRs and high-affinity nicotinic binding sites are not equivalent. FEBS Lett. 205:265–268; 1986.
7. Lipiello, P. M.; Fernandes, K. G. The binding of L-[^{3}H]nicotine to a single class of high affinity sites in rat brain membranes. Mol. Pharmacol. 29:448–454; 1986.
8. Lowry, O. H.; Rosebrough, N. J.; Farr, A. L.; Randall, R. J. Protein measurement with the Folin phenol reagent. J. Biol. Chem. 193: 265–275; 1951.
9. Lukas, R. J. Properties of curaremimetic neurotoxin binding sites in the rat central nervous system. Biochemistry 23:1152–1160; 1984.
10. Marks, M. J.; Burch, J. B.; Collins, A. C. Effects of chronic nicotine infusions on tolerance development and cholinergic receptors. J. Pharmacol. Exp. Ther. 226:806–816; 1983.
11. Marks, M. J.; Burch, J. B.; Collins, A. C. Genetics of nicotine response in four inbred strains of mice. J. Pharmacol. Exp. Ther. 226:291–301; 1983.
12. Marks, M. J.; Collins, A. C. Characterization of nicotine binding in mouse brain and comparison with the binding of α-bungarotoxin and quinuclidinyl benzilate. Mol. Pharmacol. 22:554–564; 1982.
13. Marks,M. J.; Stitzel, J. A.; Collins, A. C. Time course study of the effects of chronic nicotine infusion on drug response and brain receptors. J. Pharmacol. Exp. Ther. 235:619–628; 1985.
14. Marks, M. J.; Stitzel, J. A.; Collins, A. C. A dose-response analysis of nicotine tolerance and receptor changes in two inbred mouse strains. J. Pharmacol. Exp. Ther. 239:358–364; 1986.
15. Marks, M. J.; Stitzel, J. A.; Collins, A. C. Genetic influences on nicotine responses. Pharmacol. Biochem. Behav. 33(3):667–678; 1989.
16. Marks, M. J.; Stitzel, J. A.; Romm, E.; Wehner, J. M.; Collins, A. C. Nicotinic binding sites in rat and mouse brain: Comparison of acetyl choline, nicotine, and α-bungarotoxin. Mol. Pharmacol. 30: 427–436; 1986.
17. Martino-Barrows, A. M.; Kellar, K. J. [^{3}H]Acetylcholine and [^{3}H]-(−)-nicotine label the same recognition site in rat brain. Mol. Pharmacol. 31:169–174; 1987.
18. Miner, L. L.; Collins, A. C. Strain comparison of nicotine-induced seizure sensitivity and nicotinic receptors. Pharmacol. Biochem. Behav. 33(2):469–475; 1989.
19. Miner, L. L.; Marks, M. J.; Collins, A. C. Classical genetic analysis of nicotine-induced seizures and nicotinic receptors. J. Pharmacol. Exp. Ther. 231:545–554; 1984.
20. Miner, L. L.; Marks, M. J.; Collins, A. C. Genetic analysis of nicotine-induced seizures and hippocampal nicotinic receptors in the mouse. J. Pharmacol. Exp. Ther. 239:853–860; 1986.
21. Morley, B. J.; Kemp, G. E.; Salvaterra, P. α-Bungarotoxin binding sites in the CNS. Life Sci. 24:859–872; 1979.
22. Morrow, A. L.; Loy, R.; Creese, I. Alteration of nicotinic cholinergic agonist binding sites in hippocampus after fimbria trans section. Brain Res.334:309–314; 1985.
23. Oswald, R. E.; Freeman, J. A. Alpha-bungarotoxin binding and central nervous system nicotinic acetylcholine receptors. Neuroscience 6:1–14; 1981.
24. Romano, C.; Goldstein, A. Stereospecific nicotine receptors on rat brain membranes. Science 210:647–650; 1980.
25. Schwartz, R. D.; Kellar, K. J. Nicotinic cholinergic receptor binding sites in brain: in vivo regulation. Science 220:214–216; 1983.
26. Schwartz, R. D.; McGee, R., Jr.; Kellar, K. J. Nicotinic cholinergic receptors labeled by [^{3}H]acetylcholine in rat brain. Mol. Pharmacol. 22:56–62; 1982.
27. Sershen,H.; Reith, M. E. A.; Lajtha, A.; Gennaro, J., Jr. Noncholinergic saturable binding of (±)-[^{3}H]nicotine to mouse brain. J. Recept. Res. 2:1–15; 1981.
28. Whiting, P. J.; Lindstrom, J. M. Purification and characterization of a nicotinic acetylcholine receptor from rat brain. Proc. Natl. Acad. Sci. USA 84:595–599; 1987.